Pumped Thermal Electricity Storage for Active Distribution Network Applications

Ahmad Asrul Ibrahim*
Behzad Kazemtabrizi
Chiara Bordin
School of Engineering and Computing Sciences
Durham University
Durham, United Kingdom
*e-mail: a.a.ibrahim@durham.ac.uk

Chris J. Dent
School of Mathematics
University of Edinburgh
Edinburgh, United Kingdom

Joshua D. McTigue
Alexander J. White
Department of Engineering
University of Cambridge
Cambridge, United Kingdom

***Abstract*—This paper introduces a new model for Pumped Thermal Electricity Storage (PTES) devices as an emerging thermal storage technology. PTES devices are capable of reaching higher capacities than battery storage devices and therefore are suitable for grid-scale storage at the distribution voltage levels. The new model captures the inherent thermal characteristics, such as the variable efficiency, of the PTES device, yet it is not computationally burdensome for integration into non-linear optimisation problem formulations. It therefore makes it suitable for operational planning studies in active distribution networks. The new model uses a two-stage regression of a detailed thermodynamic model of PTES to capture the approximate behaviour. The salient feature of this reduced model is that the variable efficiency is a function of the energy content – the state of charge – of the device. The new model is tested on a medium-voltage 33-bus distribution network within a dynamic optimal power flow formulation for day-ahead operational planning. The main objective has been to minimize daily cost of buying energy from the external grid. The results have been compared with the same test network without any storage devices and with storage models with fixed round-trip efficiency. In both cases the results clearly show the suitability and prowess of the new model in producing accurate operational cycles for the device and its benefits in terms of significant savings in operational costs when using large-scale PTES devices.**

***Index Terms*—Active distribution network; dynamic optimal power flow; energy management framework; pumped thermal electricity storage**

I. INTRODUCTION

An effective way of increasing the levels of electricity generation from renewable resources is integration across both transmission and distribution (in form of distributed generation resources) voltage levels within a given power system. However, their inherent intermittent behavior is potentially problematic which is why there has been a gradual paradigm toward a more active distribution network management schemes in recent years. Under the active paradigm, distribution network operators (DNOs) perform the role of system operators by coordinating control actions of both own assets (e.g. storage devices, power flow controllers) and consumer DG outputs as well as flexible demand whilst adhering to a minimum cost solution [1]. Energy Storage Systems (ESSs) are one of the many ways to enable a seamless transition from a passive network paradigm to an active one. The primary role of the ESS within a medium voltage (MV) network is to provide an alternative for the load-following mechanism and reduce dependence on the power plants (produce carbon dioxide emission) from the grid.

There have been several works exploring the benefits of ESS integration for active distribution network (ADN) applications, which range from planning (both short and long term) to technology focused [2-7]. Gill et al. [2] propose a short-term operational planning framework using a dynamic optimal power flow (DOPF) formulation for integrating inter-temporal coupling of ESS devices. The framework considers the demand flexibility (e.g. demand-side management) and non-firm DGs connection principles. On the other hand, ESS benefits have been investigated in detail at different settings including storage capacity, installation configuration, and technology efficiency [3]. Regarding the installation configuration, the study in [4] compares centralized (single large storage capacity) and distributed (multiple small storage capacity) for the day-ahead electricity market. Energy is stored in ESS when the energy price is low or there is high generation from DGs and discharged later when the price is high or there is high demand due to low DG output. The energy price arbitrage is further investigated in [5] to take advantage of ESS deployment to reduce rapid fluctuations in the solar generation and shift energy to when it is most beneficial. A similar approach is applied in [6] to stabilize the wind generation power output at maximum ESS's life span. Recently, Jayasekara et al. [7] address long-term planning issues of ESS including placement and sizing to increase hosting capacity for both solar and wind generations.

Although various types of storage technology are available, the battery storage is typically used in most of the works for ADN applications. Large-scale storage technologies

This work was funded by EPSRC grants (EP/J006297/1, EP/J006296/1 and EP/K00252/1). Ahmad Asrul Ibrahim is sponsored by Universiti Kebangsaan Malaysia and Ministry of Higher Education's Malaysia.

such as the pumped hydro storage (PHS) and compressed air storage (CAS) are limited to geographical constraints and are not suitable for integration to most MV networks. Thermal energy storage (TES) is a potential alternative to both battery storage and PHS/CAS as it does not have the geographical limitations of the latter and has low capital cost per kWh at a very long life cycle [8]. Many different materials can be used in TES, such as water, molten salts and concrete. A Pumped Thermal Electricity Storage (PTES) employs packed beds filled with pebbles and consequently exhibits lower environmental damage than batteries which contain toxic chemicals [9]. Despite all the advantages, the possibility of using TES for ADN applications is yet to be thoroughly investigated. This paper develops an analytical framework for modelling a PTES system, based on the work presented in [10-11], suitable for ADN application studies. The model is simple enough for integration into a non-linear OPF formulation and yet captures the physical characteristics of the PTES. This paper studies on the thermodynamic trip efficiency of the PTES as it cycles as directed by a centralized energy management scheme.

The paper is outlined as follows: Section II describes step-by-step procedure to establish a reduced PTES model for application in active distribution networks; the ADN energy management framework using PTES is presented in Section III; Section IV discuss the results from simulation analyses; finally, conclusion is drawn in Section V.

II. Development of the PTES Reduced Model

The PTES uses thermal energy as its storage medium via temperature difference between two thermal reservoirs (e.g. cold and hot). Fig. 1 illustrates the PTES layout to give a fundamental understanding on its working principle. During charging, an electric machine works as motor to drive two compression-expansion devices (CE and EC) by pumping heat from cold to hot reservoir. When discharging, heat is released and rotates the electric machine to work as generator, thereby generating electricity back to the network.

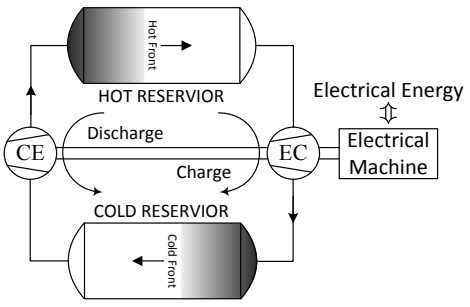

Fig. 1. PTES working principal

The internal energy losses in the ESS process (charging and discharging cycles) are normally generalized as a round-trip efficiency to give an indication of the system performance. The round trip efficiency is then used to determine the remaining energy in the storage unit for energy management purposes. The parametric losses of the PTES (i.e., pressure, temperature and other geometric factors) are discussed in detail in [10-11] to attain optimal design. In this work, through the use of a coherent computational framework a reduced model for PTES is introduced, which is suitable for non-linear OPF formulations. Fig. 2 shows an overview of how the reduced model was developed by combining various stages of modelling from detailed to reduced using three distinct computational stages.

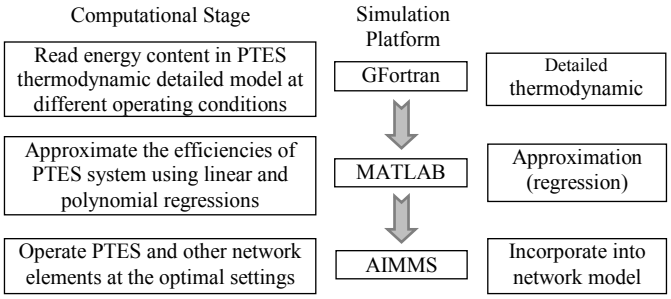

Fig. 2. Approximation and network integration procedure

A. Stored Energy and Operating Power

The available energy stored within a storage system is influenced by the charge efficiency, discharge efficiency and self-discharge. However, the amount of self-discharge is very small and can be neglected [4]. Therefore, the energy content in the storage unit can be determined using two distinct operating power states (charging and discharging) as given in the following expressions:

$$E(t+1) = E(t) + \Delta E \tag{1}$$

$$\Delta E = \eta P(t) \tau \tag{2}$$

$$\eta = \begin{cases} \eta_c, & \text{if } P(t) > 0 \\ \eta_d^{-1}, & \text{otherwise} \end{cases} \tag{3}$$

where η_c, η_d, $P(t)$ and τ are charging efficiency, discharging efficiency, operating power and time interval, respectively. The operating power state is based on generator convention where positive sign denotes charging operation and negative denotes discharging operation.

The stored energy that can be converted back into electrical energy is extracted from PTES thermodynamic detailed model to establish a model approximation based on expressions (1)-(3) by using a least-square linear regression approach. For the purpose of determining storage efficiency from the slope, the linear regression is constrained to intercept at the origin. A hypothetical 4.5 MWh PTES system at maximum power rating of 1.25 MW has been considered for developing the thermodynamic model. The following steps have been taken to create the reduced PTES model:

1) *Set an initial condition (energy level) in the storage*
2) *Charge at a given power (e.g., 125 kW) for 10 minutes*
3) *Calculate the quantity of energy that was stored in this time and the input energy (kWh). The ratio between these numbers is the charging efficiency for this power rating and initial state of charge (SoC)*
4) *Repeat steps 1) to 3) with different power ratings (e.g., using intervals of 125 kW)*
5) *Plot the stored energy against the input energy for each of these power ratings. Apply regression using*

linear least squares method and trust-region fitting algorithm in MATLAb toolbox to obtain the average efficiency for this initial state of charge

6) *Repeat steps 1) to 5) for the discharging cycle*

B. Non-linear Efficiencies

A number of physical processes act to reduce the efficiency of the PTES system as described in [11]. For instance, frictional effects cause pressure losses in valves, pipes, and along the reservoirs. Conduction and heat transfer across a finite temperature difference are thermodynamically irreversible, and these effects are particularly significant in the reservoirs. Together these losses determine the temperature distribution along the reservoirs. The temperature distribution can consequently be seen to influence both the efficiency and the state of charge. Because energy is stored thermally and needs to be converted into electricity using a heat engine, the best measure of the content of a reservoir is "exergy". Exergy is a measure of the maximum work that can be extracted from the reservoirs, and is therefore lower than the energetic SoC. Exergy provides a useful framework in which to define the various losses in efficiency as in [11].

A constant value should not be assumed for the efficiency since it depends on a number of factors, such as the state of charge, the power input/output, and temperature distributions. Furthermore, in thermal storage systems it is possible for the same SoC to be achieved with different temperature distributions in the reservoir. If the system is charged and discharged with regular cycles, the system converges on a steady-state operation whereby the temperature distributions are the same from one cycle to the next. However, steady-state operation cannot be achieved with the irregular load cycles that may occur when PTES is part of a network. As a result, the temperature distributions can change significantly, and the efficiency and state of charge of the current cycle are therefore affected by the historical operation of the system. In this work, the load cycles do not differ significantly from one another, and this dependency on the history of operation is not particularly obvious. Therefore, it is possible to simplify the PTES characteristics using simple regression techniques based on the efficiency and energetic (rather than exergetic) SoC. For highly erratic load cycles, it will be necessary to develop a simplified model which can take into account the historical operation and the exergetic content of the reservoirs.

As the reservoirs become more fully charged, the efficiency decreases. The temperature distribution along the stores has a finite gradient rather than being a step-change. As the reservoirs charge, the outlet temperature changes. For instance, during charge, the hot reservoir outlet temperature increases, causing a so-called "exit loss", and hence a reduction in efficiency. A similar process occurs during discharge. To characterize the non-linear relationship between PTES efficiency and the energetic State of Charge, the process introduced in Section II.A is repeated for different initial conditions. Finally, using nonlinear regression based on least absolute residuals approach, a polynomial expression is derived for both charge and discharge efficiencies which are shown in (4) and (5), respectively.

III. Energy Management Framework

A centralized energy management framework for day-ahead operational planning managed by the DNO is introduced in this section. Fig. 3 shows an overview of the energy management framework which aims to minimize the cost of buying electricity from the external grid supply point (GSP) through optimum ESS utilization. In this framework, DNO owns the ESS and will optimize all assets to achieve the target taking into account the costs of trading electricity with the grid supply, buying from DG owners, and supplying to consumer as illustrated in Fig. 3. Power curtailment is essential as part of the framework to avoid network constraints violation during high generation. Although energy is curtailed from the DGs, there is a cost (or equivalent) of curtailment beyond having to buy the energy elsewhere.

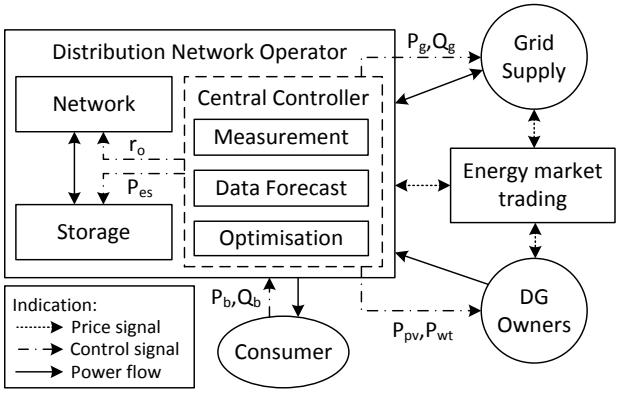

Fig. 3. Energy management architecture

The energy management framework is tested on the 33-bus benchmark test network [12] with an OLTC transformer. The total active and reactive power loads at the peak of 3.715 MW and 2.3 MVar, respectively. We assume voltage limits of 0.97/1.03 pu (±3% of the nominal voltage) at all buses and thermal limit of lines, S_{max} = 5 MVA. Two solar-based DGs and four wind-based DGs of 1 MW are considered to simulate high renewable penetrations. The two solar-based DGs are allocated at buses 13 and 18 whereas four wind-based DGs at buses 6, 7, 28 and 33. A 1.25 MW ESS unit at storage capacity of 4.3475 MWh is installed at bus 10. The price arbitrage ADN energy management framework is formulated as a non-linear DOPF as given in the appendix.

Fig. 4 depicts the time-variant of the energy market price [13], demand, wind and solar power profiles [7] in 24 hour periods for the purpose of this study. Three different case studies are considered as mentioned in Table I. It should be noted that in this paper an ESS with fixed efficiency is any storage device whose efficiency given in (3) is kept fixed. The results are analyzed in terms of energy losses, network operation that includes power exchange, tap ratio, storage unit operation and the subsequent total operational cost.

TABLE I
Case Studies

Case	Tap control	ESS control	Efficiency
No ESS	Yes	No	N/A
Fixed efficiency	Yes	Yes	Constant
PTES efficiency	Yes	Yes	Non-linear

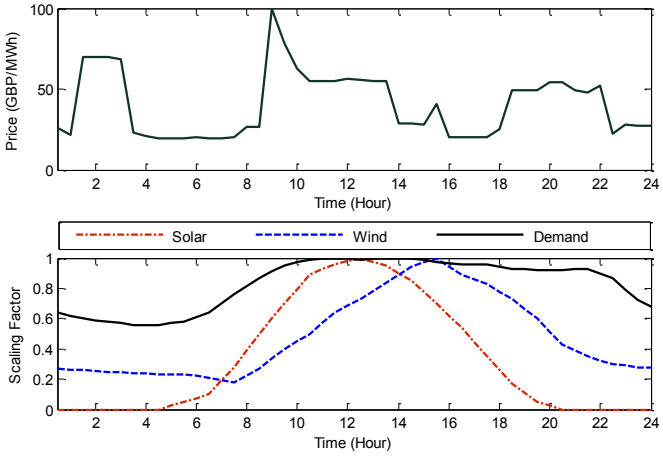

Fig. 4. Time-variant of hourly energy market price, demand, wind and solar power profiles for a day-ahead planning

IV. Numerical Results

The outcomes of the numerical simulation experiments for deriving the reduced PTES model are first presented in this section followed by its performance when integrated within the ADN energy management framework. The non-linear dynamic OPF has been formulated in AIMMS modelling environment [14] and solved using CONOPT 3.14V.

A. PTES Reduced Model: Efficiency Trends

Fig. 5 shows two examples of linear regression carried out to obtain an approximate polynomial efficiency expression. It shows that PTES stores energy at a non-linear rate as initial SoC increases. This trend is not as apparent when PTES is discharging. An overall performance of this stage regression process is indicated by sum square error (SSE), R-square and root mean square error (RMSE), respectively in average, as 8.17×10^{-4}, 0.992, and 0.41% for charging, and 2.97×10^{-3}, 0.997, and 0.75% for discharging. The results indicate that the storage efficiency is most sensitive to the power rating when "exit losses" occur, as described in section II.B. Power ratings have the greatest impact on behavior when the store has a high SoC during charge, or a low SoC during discharge.

The variations of approximated efficiencies are then plotted against the initial SoC to obtain an explicit polynomial expression for the efficiency as a function of SoC. Fig. 6 illustrates the relationships between the efficiency and SoC using the polynomial regression. A polynomial order 4 has found to be the best fit in this study after few times of regression process. As a result, the charging and discharging efficiency functions can be derived as expressed in (4) and (5). The performance of polynomial regressions in terms of SSE, R-square, RMSE are; 2.18×10^{-3}, 0.999 and 0.996%, respectively for charging, and 2.59×10^{-4}, 0.998 and 0.36%, respectively for discharging.

$$\eta_c = -6.523\times SoC^4 + 9.946\times SoC^3 - 5.458\times SoC^2 + 1.29\times SoC + 0.7683 \quad (4)$$

$$\eta_d = -1.985\times SoC^4 + 3.4\times SoC^3 - 1.988\times SoC^2 + 0.4213\times SoC + 0.9503 \quad (5)$$

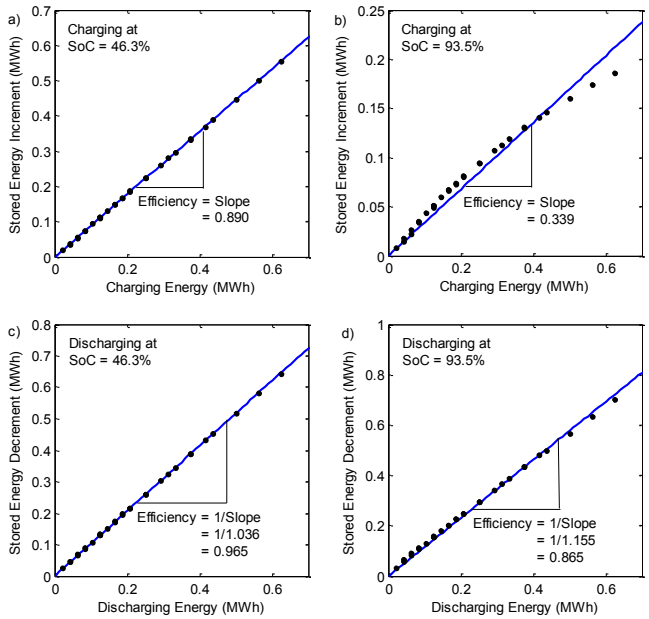

Fig. 5. Linear regression between consuming/demanding energy and changes of stored energy to determine efficiency

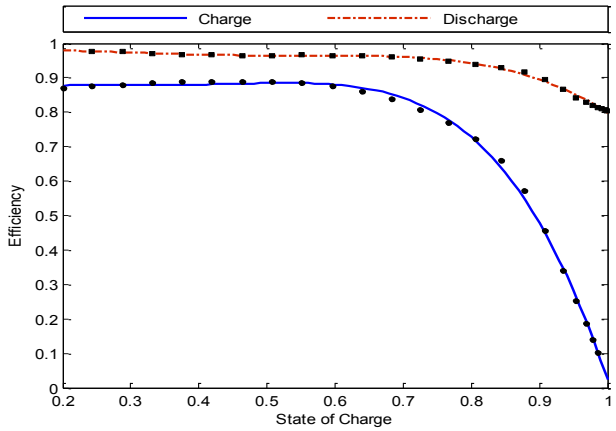

Fig. 6. Polynomial regression to obtain charging and discharging efficiency curves in state of charge terms

In order to validate the reduced model, the optimal storage scheduling is obtained from varying energy market price in standalone application without involvement of any network constraints. The optimal power cycle is then fed into thermodynamic detailed model for comparison purposes. The simulation is run for 20 days due to computational limitations of the detailed model. Fig. 7 depicts the comparison results between the reduced model and thermodynamic detailed model in terms of variations in the energy content. Based on the figure, the reduced model follows the detailed model quite closely with slight error during the idle states. This is mainly due to the fact that the detailed model includes the self-discharge in the reservoirs but as mentioned in section II.A, this is not included in the reduced model. An overall performance shows SSE and RMSE at 0.365 and 1.95%, respectively. This indicates it is acceptable to use this technique in order to simplify the PTES model for network applications without neglecting its physical characteristics.

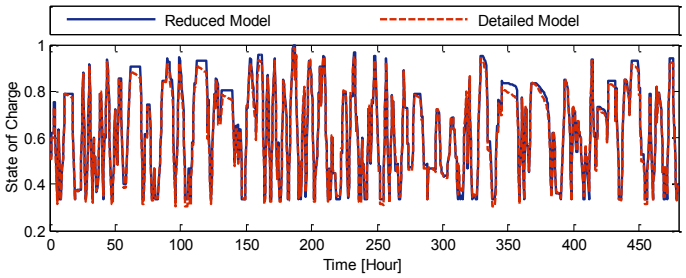

Fig. 7. A comparison between the reduced and detailed models

B. *PTES Application on MV Distribution Network*

Table II shows the summary of network operation for three cases with the objective of minimizing cost through an arbitrage process. Although ESS application shows higher line losses and power curtailment, it has gained more profit at lower costs from buying at low price and selling at high price. It is also apparent that when it comes to energy losses within the storage unit, the PTES reduced model with varying efficiency gives better performance than an ESS with a fixed efficiency of 90%. As a result, the PTES reduced model shows significant savings of more than 63% when compared to the base case (i.e. no ESS) and slightly higher than the fixed efficiency model (7.4% improved). The better performance by the PTES reduced model is precisely due to the non-linearity in the PTES charge and discharge efficiencies, which makes it rarely ever go to a very high/low charge.

TABLE II
ENERGY LOSSES AND OPERATION COST OF MINIMIZING COST

Case	Energy Losses (MWh)			Total
	Network	*Storage*	*Curtail*	Cost (£)
No ESS	4.522	N/A	2.225	587.39
Fixed efficiency	5.216	3.151	2.879	228.99
PTES efficiency	4.990	2.799	2.374	212.02

Fig. 8 depicts a comparison of daily operation between the case study without ESS, the conventional fixed efficiency model and the reduced PTES model as described in Table I. Referring to Fig. 8(a), there is minimal exchange of power in the base case with the grid supply, however both storage cases show a higher variation of power exchange due to the use of the storage device for buying energy at low price and selling at high price. The secondary voltage of the substation transformer is normally regulated at 1.03 p.u. as shown in Fig. 8(b). Nevertheless, high power injections from DGs have caused voltage rise at the connected terminals that lead to tap ratio decreases. At high price period during peak generation (between 8:30 and 10:30), ESS tends to discharge electricity that has been stored during lower price periods. Hence, DG output needs to be curtailed to avoid voltage rises as presented in Fig. 8(c). Instead, the DG surplus energy at low price periods (between hours 14 and 16) is stored by the ESS to avoid curtailment. Fig. 8 clearly shows the impact of ESS in providing a trade-off between energy price, demand and resource fluctuations for an optimum operation strategy.

The daily operation of the reduced PTES model as compared to the conventional fixed efficiency model is given in Fig. 9. There is significant different operation between the fixed and reduced PTES models between hours 3 to 7 and few other times at hours 12 and 21 as demonstrated in Fig. 9(a). It is obvious that because of the non-linear efficiency characteristics, losses will increase as PTES reduced model is fully charged or discharged. This has put a natural limit on how much PTES is charged/discharged at each point in time indicated in Fig. 9(b). Consequently, PTES reduced model almost constantly maintains a high round-trip efficiency (so operates within the normal region of the efficiency characteristic) as shown in Fig. 9(c) to maintain a minimum cost solution. Exceptions would be at hour 17 where due to low price it is worth to charge as high as possible at the expense of loss a dramatic loss in efficiency. Overall, PTES operating efficiency is slightly lower than the conventional model precisely due to the non-linear characteristic of the efficiency.

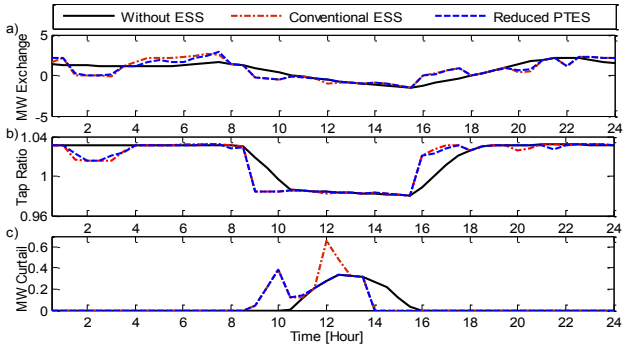

Fig. 8. A performance comparison of daily operation; a) power exchange with the grid supply, b) tap changer, c) power curtailment

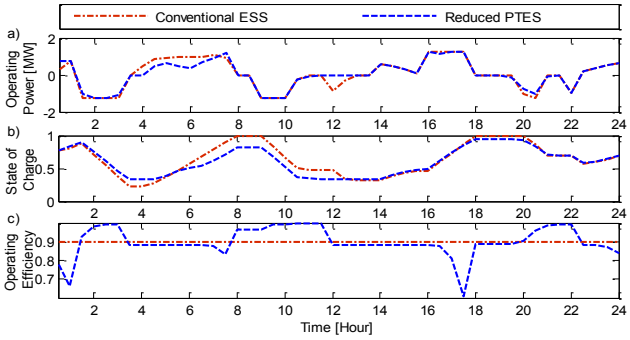

Fig. 9. A comparison of daily operation between conventional ESS and reduced PTES model; a) ESS operating power, b) state of charge, c) operating efficiency

V. CONCLUSION

This paper proposes a new variable efficiency model based on PTES characteristics for day-ahead operational planning in active distribution networks. The ESS charging/discharging efficiency is derived using two-stage regression technique; 1) linear regression to obtain efficiency at any operating power, and 2) polynomial regression to attain the variable efficiency as function of SoC. The established PTES model is evaluated to show that it operates according to the thermodynamic detailed model with a minute error due to the inclusion of reservoir self-discharge in the detailed model. This indicates the PTES can successfully be represented into a reduced form

suitable for power system operational planning studies. An AC DOPF formulation is applied on the 33-bus test network to showcase the performance of the PTES model for energy management application as compared to the conventional model based on fixed efficiency. In the network operation, the PTES operates at slightly different points with better performance than the fixed 90% efficiency ESS model. Due to the nonlinearity of the PTES efficiency it will not fully charge as the efficiency drops at higher levels of SoC. Overall, the PTES reduced model has provided a better representation of PTES characteristics that would be beneficial for accurate assessments of large-scale thermal storage integration and operational planning in active distribution networks.

REFERENCES

[1] S. Gill, I. Kockar and G.W. Ault, "Dynamic optimal power flow for active distribution networks," *IEEE Transactions on Power Systems*, vol. 29, no. 1, pp. 121–131, January 2014.

[2] S. Carr, G.C. Premier, A.J. Guwy, R.M. Dinsdale and J. Maddy, "Energy storage for active network management on electricity distribution networks with wind power," *IET Renewable Power Generation*, vol. 8, no. 3, pp. 249–259, 2014.

[3] M. Parvania, M. Fotuhi-Firuzabad and M. Shahidepour, "Comparative hourly scheduling of centralized and distributed storage in day-ahead market," *IEEE Transactions on Sustainable Energy*, vol. 5, no. 3, pp. 729–737, July 2014.

[4] A. Nagarajan and R. Ayyanar, "Design and strategy for the deployment of energy storage systems in a distribution feeder with penetration of renewable resources," *IEEE Transactions on Sustainable Energy*, vol. 6, no. 3, pp. 1085–1092, July 2015.

[5] F. Luo, K. Meng, Z. Y. Dong, Y. Zheng, Y. Chen and K. P. Wong, "Coordinated operational planning for wind farm with battery energy storage system," *IEEE Transactions on Sustainable Energy*, vol. 6, no. 1, pp. 253–262, January 2015.

[6] N. Jayasekara, M. A. S. Masoum and P. J. Wolfs, "Optimal operation of distributed energy storage systems to improve distribution network load and generation hosting capability," *IEEE Transactions on Sustainable Energy*, vol. 7, no. 1, pp. 250–261, January 2016.

[7] H. Chen, T. N. Cong, W. Yang, C. Tan, Y. Li and Y. Ding, "Progress in electrical energy storage system: A critical review," *Progress in Natural Science*, vol. 19, pp. 291–312, 2009.

[8] M. C. McManus, "Environmental consequences of the use of batteries in low carbon systems: The impact of battery production," *Applied Energy*, vol. 93, pp. 288–295, 2012.

[9] T. Desrues, J. Ruer, P. Marty and J. F. Fourmigué, "A thermal energy storage process for large scale electric applications," *Applied Thermal Engineering*, vol. 30, pp. 425–432, 2010.

[10] A. White, G. Parks and C. N. Markides, "Thermodynamic analysis of pumped thermal electricity storage," *Applied Thermal Engineering*, vol. 53, pp. 291–298, 2013.

[11] J.D. McTigue, A. White and C.N. Markides, "Parametric studies and optimisation of pumped thermal electricity storage," *Applied Energy*, vol. 137, pp. 800–811, 2015.

[12] M. E. Baran and F. F. Wu, "Network reconfiguration in distribution systems for loss reduction and load balancing," *IEEE Transactions on Power Delivery*, vol. 4, no. 2, pp. 1401–1497, 1989.

[13] ELEXON Ltd. *NETA: Balancing Mechanism Reporting System* [Online]. Available: www.bmreports.com/bwx_home.htm [Access on 13 June 2016]

[14] J. Bisschop and M. Roelofs. *AIMMS Language Reference, Version 3.12*. Haarlem, Netherlands: Paragon Decision Technology, 2011.

APPENDIX

Let *N*, *PV*, *WT*, *G*, *E*, *L*, *T*, *C*, and *M* denote the sets of respectively, nodes, solar-based DGs, wind-based DGs, grid supply points (GSPs), storage units, power lines, the subset of lines with on-load tap changer (OLTC) transformers, and time periods. The full optimal operation planning in period *t* is formulated as a full AC dynamic optimal power flow problem as such:

$$\min\left\{\sum_{t\in M}\sum_{g\in G} c(t)P_g(t)\tau\right\} \tag{6}$$

$$P_g^{\min} \le P_g(t) \le P_g^{\max} \qquad \forall g \in G \tag{7}$$

$$Q_g^{\min} \le Q_g(t) \le Q_g^{\max} \qquad \forall g \in G \tag{8}$$

$$0 \le P_{pv}(t) \le P_{ava,pv}(t) \qquad \forall pv \in PV \tag{9}$$

$$0 \le P_{wt}(t) \le P_{ava,wt}(t) \qquad \forall wt \in WT \tag{10}$$

$$P_e^{\min} \le P_e(t) \le P_e^{\max} \qquad \forall e \in E \tag{11}$$

$$SoC_e(t+1) = SoC_e(t) + \eta_e(t)\,P_e(t)\tau \big/ E_e^{\max} \qquad \forall e \in E \tag{12}$$

$$\eta_e(t) = \begin{cases} \eta_{c\{e\}}(t), & \text{if } P(t) > 0 \\ \eta_{d\{e\}}^{-1}(t), & \text{otherwise} \end{cases} \qquad \forall e \in E \tag{13}$$

$$SoC_e^{\min} \le SoC_e(t) \le SoC_e^{\max} \qquad \forall e \in E \tag{14}$$

$$SoC_e(t_{final}+1) = SoC_e(t_{start}) \qquad \forall e \in E \tag{15}$$

$$\alpha_o^{\min} \le \alpha_o(t) \le \alpha_o^{\max} \qquad \forall o \in T \tag{16}$$

$$V_g(t) = 1 \qquad \forall g \in G \tag{17}$$

$$\theta_g(t) = 0 \qquad \forall g \in G \tag{18}$$

$$V_{\min} \le V_b(t) \le V_{\max} \qquad \forall b \in N \tag{19}$$

$$\overline{S}_{sn\{l\}}(t) = \overline{Y}_l^{*}[(V_{sn\{l\}}(t))^2 - (\overline{V}_{sn\{l\}}(t))(\overline{V}_{rn\{l\}}(t))^{*}] \qquad \forall l \in L \tag{20}$$

$$\overline{S}_{rn\{l\}}(t) = \overline{Y}_l^{*}[(V_{rn\{l\}}(t))^2 - (\overline{V}_{sn\{l\}}(t))^{*}(\overline{V}_{rn\{l\}}(t))] \qquad \forall l \in L \tag{21}$$

$$(S_{sn,rn\{l\}}(t))^2 \le S_{\max}^2 \qquad \forall l \in L \tag{22}$$

$$\begin{aligned} &P_{g\{b\}}(t) + jQ_{g\{b\}}(t) + P_{pv\{b\}}(t) + P_{wt\{b\}}(t) + P_{e\{b\}}(t) \\ &= P_{d\{b\}}(t) + jQ_{d\{b\}}(t) + \sum_{l\in L|sn=b}\overline{S}_{sn\{l\}}(t) + \sum_{l\in L|rn=b}\overline{S}_{rn\{l\}}(t) \end{aligned} \tag{23}$$

The objective function is given by (6) to minimize cost of buying energy from the grid supply depending on the energy market price, $c(t)$ with τ time-interval. The active and reactive power limits that flow through the primary substation transformer are given by (7) and (8). The operating boundary of DGs in (9) and (10) are used to correlate with the available resources (e.g. solar and wind). There is no reactive power injection from the DGs as they are assumed to operate at unity power factor. Constraint (11) provides the operating power limits of the ESS unit. State of charge (SoC) is updated over time using expressions (12) and (13) that should be within a boundary as given in (14). Energy balance constraint in (15) is imposed to avoid the storage unit from produce or consume additional energy. Equations (16)–(18) give constraints on the tap changer ratio, α and voltage magnitude/angle for the slack bus (the grid supply point).The statutory voltage limits for all buses are defined in (19). The complex power flow equations for lines at sending and receiving ends are expressed in (20) and (21), respectively. The thermal limits of lines as given in (22) must be obeyed at all the times. According to Kirchhoff's current law, power injections at each bus are ensured to be balance using (23).